J. Fluid Mech. (1975), *vol.* 71, *part* 2, *pp.* 231–240
Printed in Great Britain

Convection in boxes: an experimental investigation in vertical cylinders and annuli

By K. STORK AND U. MÜLLER
Lehrstuhl für Strömungslehre, Universität Karlsruhe, Germany

(Received 25 February 1974 and in revised form 9 December 1974)

Convective flow of the cellular type has been investigated in vertical cylinders of axisymmetric and annular shape. The critical Rayleigh numbers were determined as functions of the box diameter and the gap width respectively. A distinct influence of side walls with different thermal conductivities was observed.

1. Introduction

Free convection in horizontal fluid layers has been counted among the classical problems of hydrodynamic stability since the phenomenon of cellular convection studied by Bénard (1900) first received a theoretical treatment by Rayleigh (1916). This so-called Rayleigh–Bénard problem has since been frequently investigated experimentally and theoretically (see, for example, the survey article of Koschmieder 1974).

Though formerly the fluid layers have usually been assumed to have infinite horizontal extent and simulated accordingly in experiments, several recent investigations of the influence of side walls on the onset of convection have been performed. Most cases were concerned with convective flow in boxes of rectangular shape (e.g. Davis 1967; Stork & Müller 1972). The present article may be considered as an extension of the experimental work reported in Stork & Müller (1972, hereafter termed part 1). The previous results on the onset of convection in rectangular vessels have been extended to boxes of axisymmetric shape. Experiments in vessels of circular shape and large extent have been performed by Koschmieder (1966*a*, *b*). The present results are compared with the calculations of Charlson & Sani (1970, 1971) as well as those of Liang, Vidal & Acrivos (1969) for circular vessels.

2. Experimental apparatus and procedure

For the experiments an improved version of the apparatus described in part 1 was used. The fluid layer was enclosed between a 10 mm thick copper plate and a 4 mm thick glass plate. A thermostatically controlled water bath provided a uniform temperature distribution on each plate. In order to ensure good visibility of the fluid flow the cooling water was circulated over the glass plate through two inlets and one enlarged outlet at the periphery of the cooling

	M 300	M 200	Dimensions
ρ	$0{\cdot}994 - 8{\cdot}97 \times 10^{-4} \times T$	$0{\cdot}992 - 9{\cdot}91 \times 10^{-4} \times T$	g cm^{-3}
ν	$590 \times \exp(-0{\cdot}017 \times T)$	$306 \times \exp(-0{\cdot}017 \times T)$	cm^2 s^{-1}
β	$8{\cdot}97 \times 10^{-4}$	$9{\cdot}91 \times 10^{-4}$	grad^{-1}
λ	$0{\cdot}1416 \times 10^{-4} \times T$	$0{\cdot}1416 \times 10^{-4} \times T$	kcal m^{-1} h^{-1} grad^{-1}
c	0·36	0·36	kcal kg^{-1} grad^{-1}

TABLE 1. Properties of silicon oils ($0 \leqslant T \leqslant 100°$ C). ρ is the density, ν the kinematic viscosity, λ the thermal conductivity, β the thermal coefficient of volumetric expansion, c the specific heat and T the average temperature of the fluid in °C.

section (see part 1, figure 1). A cooling-water flow rate of 17 l/min was used. Compared with the first version of the apparatus this is an increase of nearly 70 %. The reason for increasing the flux of cooling water was to achieve as uniform a temperature distribution as possible at the top of the fluid. A fluid layer of depth 10 mm was employed. Frames of circular shape were inserted into the layer, forming a closed space with the upper and lower plate. The convective flow in this space was then investigated. The temperature difference was measured with four ferro-constantan thermocouples of diameter 0·3 mm, which were fastened to the upper and the lower plate near the side wall. Two different silicon oils, M 200 and M 300, were used as test fluids. These oils had the properties given in table 1. Aluminium powder was added to the fluid as a tracer.

The temperature gradients were generated by heating the fluid from below while keeping the temperature constant on the upper plate. Experiments were performed for different ratios h/d of the box diameter h to the depth d of the fluid layer. This ratio was varied in the range $1{\cdot}4 \leqslant h/d \leqslant 6{\cdot}4$. In addition, the convective flow in annuli was studied in order to make a comparison with the results for convection in rectangular boxes given in part 1. For this purpose concentric circular plates with outer radius r_o were inserted into the circular boxes, with inner radius r_i. A detailed investigation was performed with a constant ratio $r_m/d = 4$, where $r_m = \frac{1}{2}(r_i + r_o)$. The dimensionless gap width s/d of the annulus was varied in the range $0{\cdot}6 \leqslant s/d \leqslant 3{\cdot}4$.

The critical Rayleigh number was determined by observing the onset of convective flow and reading the corresponding temperature differences from the thermocouples (for details see part 1). The number of cells and the shape of the convection pattern were observed in the critical state as well as after the critical temperature gradient had been exceeded. Most experiments were performed within boxes whose side walls consisted of a polyvinyl chloride (PVC) material, but some additional tests were carried out with side walls of brass in order to investigate the influence of wall materials of different thermal conductivities on the convection.

When investigating the convection in circular boxes a special PVC material having nearly the same heat conductivity as the silicon oil was mostly used for the side walls. The reason for such a special choice will be discussed later. During these tests the side walls were formed by frames of circular shape which

filled the gap between the warm and cool plates completely except for the circularly shaped test section. The ratio w/d of the side-wall thickness w to the layer depth d was always larger than 6, thus providing a much higher thermal resistance in the horizontal than in the vertical direction.

The experiments in annular boxes were carried out under similar conditions. Here the side-wall thickness w depends on the mean radius r_m and the gap width s. For simplicity we shall henceforth refer to the width-to-depth ratios as h, w, s and r_m.†

The tests lasted for up to seven hours. The critical state was usually reached after slowly increasing the temperature of the copper plate for about 3 h.

3. Comments on the boundary conditions

In theoretical treatments of convection flow in vessels, the steady state of pure heat conduction in the vertical direction is usually assumed as the initial state prior to the onset of convection (see Liang *et al.* 1969; Joseph 1971; Charlson & Sani 1970, 1971). Before the convection starts, a linear temperature distribution is supposed to exist within the rigid boundaries as well as in the fluid regardless of the thermal properties of the materials. Any temperature gradients in the horizontal direction are supposedly excluded and must be avoided experimentally.

Experimental difficulties in achieving such a state may arise if the vertical thermal resistance of the lateral boundary is concentrated in the gaps between the side walls of the boxes and the upper or lower plate. Such a temperature distribution results in a temperature difference between the wall and the fluid. This in turn generates a horizontal temperature gradient, which induces convective motion before the critical temperature difference between top and bottom is reached. In order to avoid such inhomogeneities, in most of our experiments the coefficients of heat conductivity of the fluid and the side walls were arranged to be nearly equal. This was achieved by the choice of a special PVC material for the side walls whose thermal conductivity is $\lambda = 0{\cdot}126$ kcal m^{-1} h^{-1} $grad^{-1}$ (that of silicon oil being $\lambda = 0{\cdot}140$ kcal m^{-1} h^{-1} $grad^{-1}$).

The strong influence of horizontal temperature gradients on the onset of convection and the flow pattern is demonstrated by some experiments in which side walls of brass in direct contact with the copper bottom were used.

4. Evaluation of the measurements and error analysis

The quantitive evaluation of the experimental data is the same as in part 1. The definition of the Rayleigh number is

$$Ra \equiv g\beta\Delta T d^3 c\rho/\lambda\nu,$$

where g is the acceleration due to gravity, β the thermal coefficient of volumetric expansion of the liquid, ΔT the temperature difference between the

† Thus h represents h/d, etc.

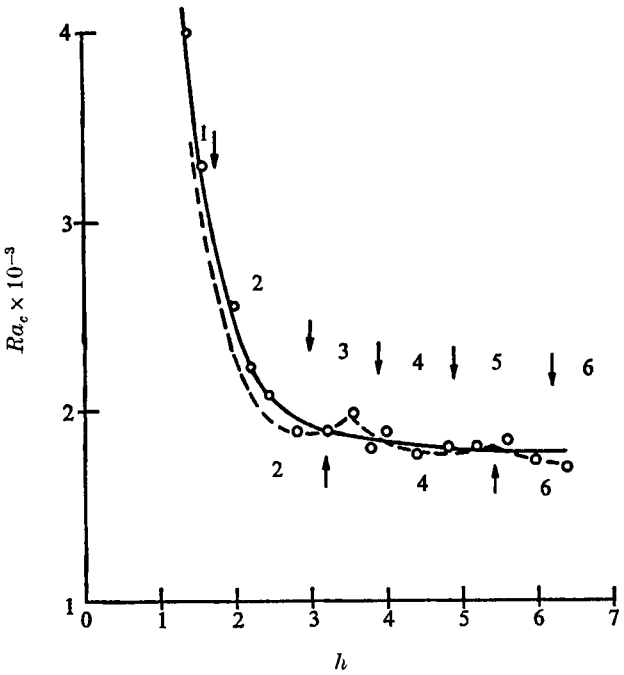

FIGURE 1. Critical Rayleigh numbers in axisymmetric boxes *vs.* box diameter h (insulating side walls, box height $d = 10$ mm). - - -, theory, Charlson & Sani; —o—, experimental results. (Error bound $|\Delta Ra_c|/Ra_c = 7\ \%$.) The numbers below and above the curves and the arrows mark the ranges of the different roll numbers. Below, theory, ring rolls (2 means 1 ring roll, 4 means 2 ring rolls, etc.); above, experiments, parallel rolls.

upper and lower plate, d the layer thickness, λ the thermal conductivity, ν the kinematic viscosity, c the specific heat and ρ the density. For ρ, λ and ν, which are generally dependent on the local temperature, mean values were used to determine the critical Rayleigh number.

As the experimental conditions were the same as in part 1, the error analysis for the critical Rayleigh number given there applies to the present investigations. Thus the critical Rayleigh number may contain a random error of up to 7 %.

5. Results and discussion

5.1. *Circular vessels*

In figure 1 the measured values of the critical Rayleigh number are plotted *vs.* the box diameter. The experimental results, given by the circles and the fitted (solid) curve, refer to vessels with side walls of large horizontal thickness ($6 \leqslant w \leqslant 10$). In this case the lateral boundaries provide nearly perfect thermal insulation. The steep slope of the curve in the lower range of box diameters and the flattening to a nearly constant value of about $Ra_c = 1800$ in the upper range characterize the influence of rigid lateral boundaries. The numbers above the curves refer to the number of roll-like cells observed under critical conditions. The arrows mark the ranges of the different numbers of rolls.

It seems reasonable to compare the experimental results with the calculation of Charlson & Sani (1970, 1971) for bounded cylindrical fluid layers. The dashed curve in figure 1 shows their results for containers with cylindrical symmetry and insulating lateral walls. The numbers below the curves refer to the number of axisymmetric ring rolls predicted by the theory. At first glance there seems to be good agreement between the experimental and theoretical values if the overall error bounds for the experiments are taken into account.

However the flow pattern observed in the experiments for diameter-to-depth ratios $h > 3{\cdot}2$ consists in most cases of rolls parallel to the diameter (see figures 2*d–g*, plate 1). This is in contrast to the axisymmetric cell pattern that is related to the theoretical curve in figure 1. Thus for this range a comparison seems doubtful because of the different cell configurations. In an extension of their 1970 work Charlson & Sani (1971) have included non-axisymmetric cell patterns. These calculations show that for aspect ratios $h > 3$ the critical Rayleigh numbers of the non-axisymmetric and axisymmetric states are fairly close together. In addition the critical Rayleigh numbers of the non-axisymmetric case may even remain slightly below the corresponding axisymmetric values for some 'patches' of the aspect ratio. Therefore within the accuracy of the measurements agreement between the observed and calculated values of Ra_c can be claimed even in the range $h > 3{\cdot}2$ if the observed pattern of parallel rolls is understood as a superposition of all types of axisymmetric and non-axisymmetric modes.

Typical cell configurations near the critical state in circular boxes can be seen in figure 2 (plate 1). For aspect ratios $h < 1{\cdot}6$ in most cases a single convection roll formed from the beginning (see figure 2*a*). These rolls usually divided up into two parts (see figure 2*b*) if the heating was continued slightly above the critical temperature difference (about 5–10% above ΔT_c), thus demonstrating that the single-roll regime is only conditionally stable against finite amplitude disturbances. In one case ($h = 1{\cdot}6$) the development of a double-roll system was observed, each roll forming a semicircle. However this state did not prove to be stable either, as one roll vanished about 7 min after its formation and the other roll then shifted to the middle of the vessel. After this, at a slightly higher temperature difference the transition to a two-cell system started as before. Charlson & Sani (1971) in their investigation predicted a two-cell pattern for vessels of diameter $d < 1{\cdot}6$ which is described by an eigenfunction of order one for the radial as well as the azimuthal co-ordinate ($J_1(\alpha\gamma r)e^{i\phi}$). With respect to this agreement between theory and experiments can only be stated conditionally. Complete agreement, however, is found for the range $1{\cdot}8 \leqslant h \leqslant 3{\cdot}2$, for both theory and experiment show that at the onset of convection a single ring roll appears (see figure 2*c*).

The orientation of the vortex rolls was either up or down in the centre. This observation is in accordance with that of Liang *et al.* (1969) and is also suggested by the theory of Müller (1965) and that of Joseph (1971).

If the dimension of the vessel is increased further, a single ring roll does not seem to be adapted to the size of the diameter, as its cross-section would become increasingly elongated with respect to the horizontal direction. The system

reacts to this by forming a single ring roll, whose position depends on the position of the first rising plume at the onset of convection. If the heating is not changed this ring roll induces after some time another convection roll near the side wall, and itself shifts away from the centre of the vessel. This configuration can be seen in figures 2(*d*), 3(*a*) and 3(*b*) (plates 1 and 2). The pattern in figure 2(*e*) may be explained in a similar way. A single ring roll near the centre induces two side rolls, and all three develop together into a parallel four-roll system (see figures 3*c*, *d*, plate 2). The same pattern can be built up in a different way. For instance in some experiments two non-concentric ring rolls appeared at the beginning of the convective flow (see figures 3*e*, *f*, plate 2). This initial condition again resulted in the same pattern as that in figure 2(*e*). However, the circulations of the different rolls were of course in opposite directions. The cell configurations in figures 2(*f*) and (*g*) developed in a similar way, before their final state was reached. Summarizing the observations for vessels of diameter $h > 3{\cdot}2$ so far, one can see that the convective flow starts near the centre of the vessel and spreads to the side wall. The influence of the side wall is relatively limited, and does not reach further than one cell diameter into the interior of the vessel. One should however keep in mind that the situation can be different when convection induced by small horizontal temperature gradients starts at the side walls and induces more and more ring rolls towards the centre as in case of a brass side wall (see figures 4*a–c*, plate 3).

The calculations of Charlson & Sani (1971) predict single ring rolls up to diameter-to-depth ratios of $h = 3{\cdot}5$ and two concentric ring rolls for $3{\cdot}5 \leqslant h \leqslant 5{\cdot}2$. For even higher values of h three-dimensional modes become increasingly important, but the calculations in this range are too incomplete with respect to higher-order modes to draw final conclusions. In order to gain more insight into the formation of the different cell patterns and their relative stability, the following tests were made in the parameter range $h > 3{\cdot}2$.†

Small lumps of soft solder (diameter 1–3 mm) were inserted at the centre of the bottom of the vessels, thus fixing the onset of convection at the middle of the box. The strength of the first rising plume and therefore the strength of the initial convection was regulated by using smaller or larger lumps of solder. By this procedure the range of a single ring roll could be artificially extended on the one hand, while on the other, two concentric ring rolls could also be generated. With respect to the strength of the initial convection, the ring-roll system at $h = 4{\cdot}4$ proved to be the relatively most stable configuration (see figures 3*g*, *h*). At a ratio $h = 5{\cdot}2$, where according to the theory three or more concentric ring rolls could be expected, ring-roll systems did not prove to be stable in a long run; rather the ring-roll system developed at a constant heat rate into a parallel roll pattern similar to that in figures 2(*f*) and (*g*) in spite of the

† In an extension of their previous work Charlson & Sani (1975) have calculated finite amplitude axisymmetric thermoconvective flows in a bounded cylindrical layer of fluid employing a Galerkin method. One of their main results is that axisymmetric states are not very stable for larger aspect ratios and at slightly supercritical Rayleigh numbers. Though referring mostly to the case of a conducting side wall, these results strongly support the observations of the present authors that for larger aspect ratios the geometry of the walls does not in general determine the cellular structure in the vessel.

pertubation centrally induced into the vessel. This development can be seen from figures 5(*a*)–(*d*) (plate 3).

One could surmise at this point that a temperature gradient in the direction of a box diameter due to the non-axisymmetric cooling device on the upper side of the fluid layer might have caused roll patterns parallel to that diameter. This objection is refuted by the following additional experiment. When the circularly shaped frames were removed from the gap and the gap was filled with the same sort of silicon oil, a system of eight completely regular concentric ring rolls could be generated by slowly heating the bottom of the layer for 3 h. This roll system, however, developed successively from the circular rim to the centre. Similar systems have been generated before by Koschmieder (1966*a*, *b*) and Pallas (1972). This indicates that the possibility of a non-axisymmetric temperature distribution, which could have induced parallel rolls (see Weber 1973), can be excluded as the frames were concentric to the gap. A further hint that temperature inhomogeneities due to non-uniform cooling were not relevant for the observed cell pattern was the fact that the orientation of the parallel roll pattern with respect to the outlet of the cooling water was random.

In order to clarify further the effect of the thermal boundary conditions on the lateral wall, some experiments were performed with frames of brass. The coefficient of heat conductivity of this material is much larger than that of the test fluid (see table 2). Generally one has to allow for the fact that a small gap filled with fluid exists between the upper plate and the side wall of the test section. The thermal resistance across this gap results in a temperature difference between the test fluid and the rigid side wall. The temperature decrease across the gap will be stronger for increasing heat conductivity of the side wall. A temperature difference between the fluid near the side wall and the side wall itself will build up and trigger convective motion in the vessel at a small subcritical Rayleigh number. For instance with brass frames first indications of convection were noticed at Rayleigh numbers $Ra \approx 200$.

In this case the convection started near the side wall in the form of a single ring roll which successively generated others until the whole inner domain was covered with a concentric roll pattern (see figure 4). This flow pattern generated by the brass wall proved to be very stable, as can be concluded from the following fact: while the two-dimensional roll patterns in a vessel with a PVC side wall are subjected to a transition to a three-dimensional pattern at a Rayleigh number about three times the critical value, no such transition process was ever observed in the case of a brass side wall even at much higher Rayleigh numbers. Details of these experiments are listed in table 1, where for comparison the corresponding values for a PVC wall are listed in addition.

5.2. *Annular containers*

So far the Rayleigh numbers at the onset of convection for circularly shaped vessels have been discussed. In the following convective flow in annuli will be described. In figure 6 the measured values of the critical Rayleigh number are plotted *vs.* the gap width. The numbers below the curve again refer to the

	PVC		Brass	
h	Ra_c	Cell configuration	Ra	Cell configuration
6·0	1800	6 parallel rolls	200	1 ring roll
			500	2 ring rolls
7·2	1760	7 parallel rolls	170	1 ring roll
			530	2 ring rolls
			1000	3 ring rolls

TABLE 2. The dependence of the Rayleigh number on the material of the side walls. λ = 0·126 and 70 kcal m^{-1} h^{-1} °C^{-1} for PVC and brass respectively

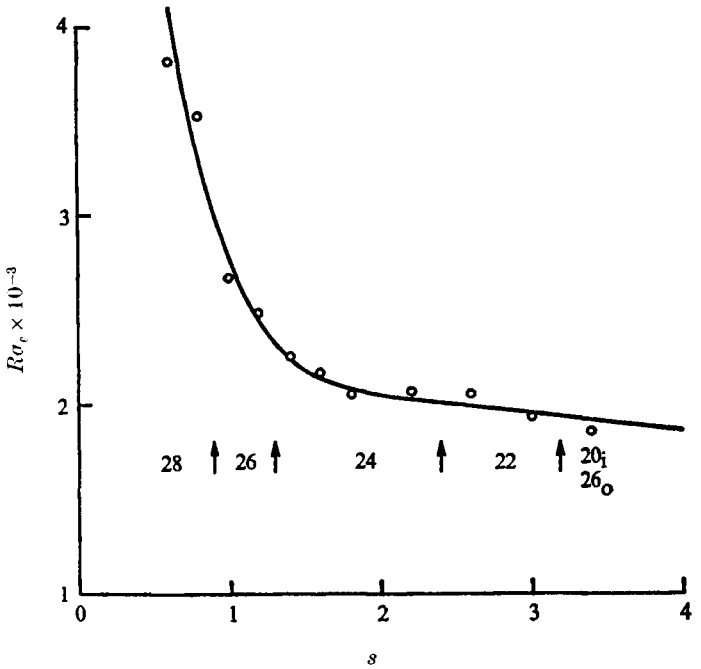

FIGURE 6. Critical Rayleigh numbers in boxes of annular shape with insulating side walls *vs.* gap width s for r_m = 4·0. (Experimental results have error bound $|\Delta Ra_c|/Ra_c$ = 7 %.) The numbers and arrows below the curve mark the ranges of the different roll numbers. The subscripts 'i' and 'o' indicate the roll numbers at the inner and outer radii respectively.

numbers of convective rolls observed and the arrows mark their ranges. For all the data plotted in figure 6 the mean radius of the annulus was constant at r_m = 4·0. The steep slope of the curve in the lower range of the gap width again characterizes the strong influence of the side walls. For larger values of the gap width the critical Rayleigh number decreases to values of about Ra_c = 1800.

Some typical cell patterns of convection flow in annuli can be seen in figure 7 (plate 4). The roll axes are directed radially and the situation is comparable to a convection pattern in a slender rectangular box whose shorter side walls are free and with the rolls parallel to the shorter side of the box. However, in the

annuli only an even number of rolls have been observed. This is in accordance with the requirement of periodicity in the azimuthal direction from a theoretical point of view. An odd number of cells would result in a shear layer between two adjacent rolls, a state which is unlikely from energy considerations.

If one assumes that at the mean radius within the gap the roll possesses a square cross-section the number of rolls should be constant for all gap sizes. For a mean radius $r_m = 4{\cdot}0$ this would result in 24 or 26 rolls. However one of these numbers of rolls was realized only in the range $1 < s < 2{\cdot}2$ (see figure 6). Twenty-eight rolls developed at values $s < 1{\cdot}0$ (see figure 7*a*). The same phenomenon of an increasing number of upward and downward convective streams with decreasing gap width has been observed in convective flow in very narrow rectangular boxes (see part 1). This effect is attributed to an enhanced dissipation, which has to be compensated by an increased release of potential energy. A more detailed description of this phenomenon is given by Davis (1967).

At higher values of s ($> 2{\cdot}5$) the difference between the lengths of the inner and outer side wall increases. Thus at a roll number of 24 or 26 in the annulus the rolls would have been strongly vertically elongated near the inner side wall and strongly horizontally elongated near the outer side wall. This would have been an unnatural and unstable situation. The experiments showed that under such conditions the system prefers a decrease in the total number of rolls around the inner side wall, but additional convective cells in the form of triangles and semicircles become embedded into the roll system near the outer side wall. This can be seen from figures 7(*e*) and (*f*). At larger gap sizes ($s > 1{\cdot}5$) the radially directed rolls became increasingly unstable near the critical condition and they divided up in the middle (see arrow in figure 7*d*) when heating at a constant temperature difference was continued for an hour or more. Similar phenomena have been observed at small gap sizes but only under definitely supercritical heating conditions. This will be discussed in more detail elsewhere.

6. Conclusions

As in the case of rectangular boxes the most evident result of the experiments on convection in circular and annular boxes is the strong decrease in the critical Rayleigh number with increasing horizontal dimension of the box. Good agreement of the critical Rayleigh numbers of the present experiments in circular boxes with the theoretical values of Charlson & Sani is obtained for insulated lateral walls. In circular vessels with diameter-to-depth ratio $d < 3{\cdot}2$ either a single roll or a ring is observed at the onset of convection. The predominant cell pattern at higher values of h consists of a system of parallel rolls. In annuli these rolls are radially directed and similar to the rolls parallel to the shorter side in rectangular boxes. Convection flow is observed at subcritical Rayleigh numbers when there is a finite heat flux through the side walls. This convection is due to temperature gradients in the radial direction. With increasing strength of this radial temperature gradient concentric ring rolls become the preferred cell pattern.

This investigation was sponsored by the Deutsche Forschungsgemeinschaft, whose financial support is gratefully acknowledged. The authors are indebted to Mr Zimmermann for valuable help during the performance of the experiments. They also appreciate the constructive criticism of one of the referees of the first version of this paper. His comments have contributed much to an improvement and better understanding of the results.

REFERENCES

BÉNARD, H. 1900 Les tourbillons cellulaires dans nappe liquide transportant de la chaleur par convection en régime permanent. *Rev. Gen. Sci. Pure Appl.* **11**, 1261–1271, 1309–1328.

CATTON, I. 1972 Effect of wall conduction on the stability of a fluid in a rectangular region heated from below. *J. Heat Transfer*, **C94**, 446–452.

CHARLSON, G. S. & SANI, R. L. 1970 Thermoconvective instability in a bounded cylindrical fluid layer. *Int. J. Heat Mass Transfer*, **13**, 1479–1496.

CHARLSON, G. S. & SANI, R. L. 1971 Thermoconvective instability in a bounded cylindrical fluid layer. *Int. J. Heat Mass Transfer*, **14**, 2157–2160.

CHARLSON, G. S. & SANI, R. L. 1975 Finite amplitude axisymmetric thermoconvective flows in a bounded cylindrical layer of fluid *J. Fluid Mech.* **71**, 209–229.

DAVIS, S. H. 1967 Convection in a box: linear theory. *J. Fluid Mech.* **30**, 465–678.

JOSEPH, D. D. 1971 Stability of convection in containers of arbitrary shape. *J. Fluid Mech.* **47**, 257–282.

KOSCHMIEDER, E. L. 1966*a* On convection on a uniformly heated plane. *Beitr. Phys. Atmos.* **39**, 1–11.

KOSCHMIEDER, E. L. 1966*b* On convection on a non-uniformly heated plane. *Beitr. Phys. Atmos.* **39**, 208–216.

KOSCHMIEDER, E. L. 1974 Bénard convection. *Adv. in Chem. Phys.* **26**, 177–211.

KOSCHMIEDER, E. L. & PALLAS, S. G. 1974 Heat transfer through a shallow horizontal convecting fluid layer. *Int. J. Heat Mass Transfer*, **17**, 991–1002.

LIANG, S. F., VIDAL, A. & ACRIVOS, A. 1969 Buoyancy-driven convection in cylindrical geometries. *J. Fluid Mech.* **36**, 239–253.

MÜLLER, U. 1965 Untersuchungen an rotationssymmetrischen Zellularkonvektionsströmungen II. *Beitr. Phys. Atmos.* **38**, 9–22.

MÜLLER, U. 1966 Über Zellularkonvektionsströmungen in horizontalen Flüssigkeitsschichten mit ungleichmäßig erwärmter Bodenfläche. *Beitr. Phys. Atmos.* **39**, 217–234.

PALLAS, S. G. 1972 Heat transfer and wavelength measurement for axisymmetric flow of a fluid heated from below. Ph.D. thesis, University of Texas, Austin.

RAYLEIGH, LORD 1916 On convection currents in a horizontal layer of fluid when the higher temperature is on the underside. *Phil. Mag.* **32**, 529–546.

STORK, K. & MÜLLER, U. 1972 Convection in boxes: experiments. *J. Fluid Mech.* **54**, 599–611.

WEBER, J. E. 1973 On thermal convection between non-uniformly heated planes. *Int. J. Heat Mass Transfer*, **16**, 961–970.

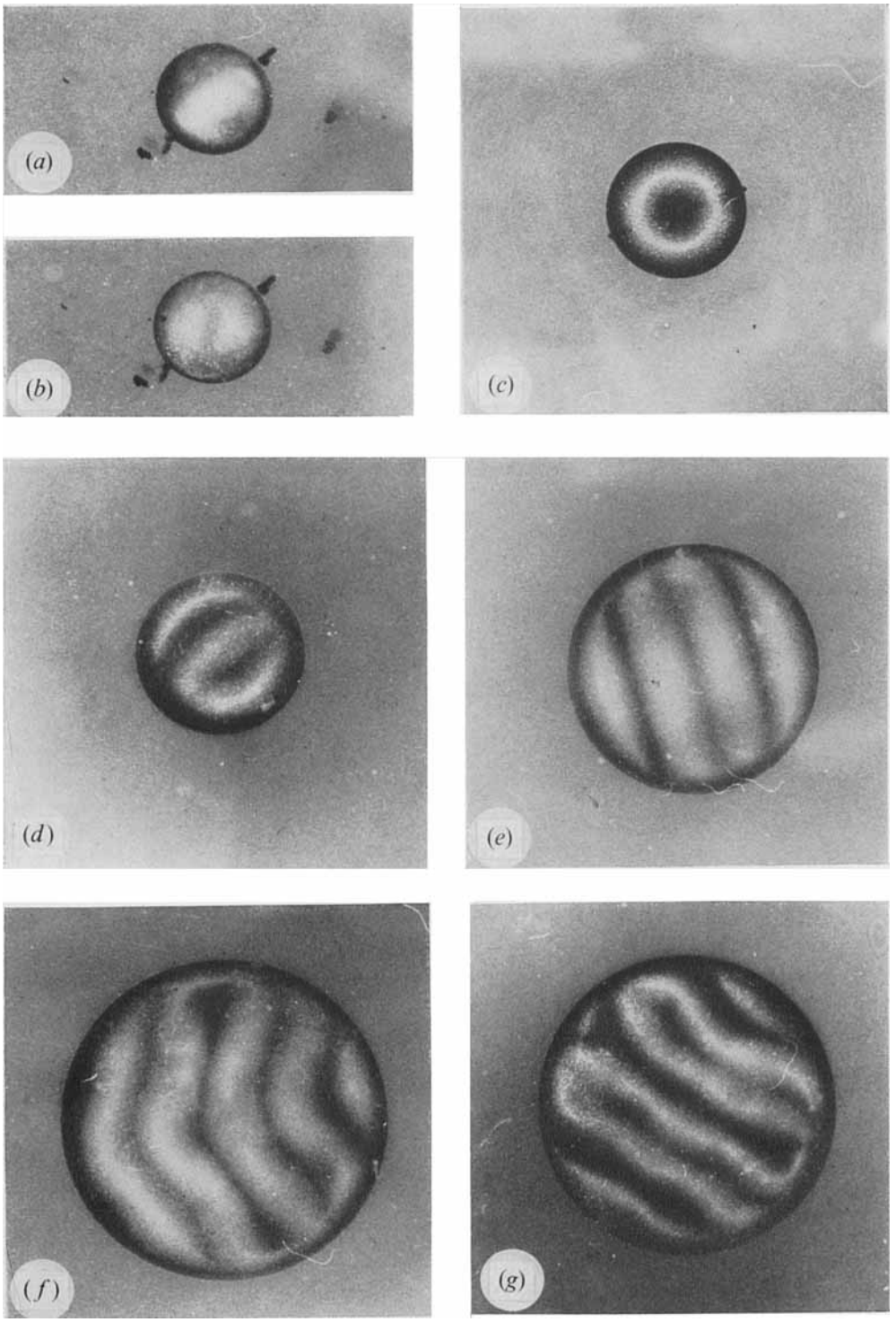

FIGURE 2. Convection rolls in axisymmetric boxes of large side-wall thickness ($w > 6$). (*a*) $h = 1{\cdot}6$, 1 roll. (*b*) $h = 1{\cdot}6$, 2 rolls. (*c*) $h = 2{\cdot}2$, 1 ring roll. (*d*) $h = 3{\cdot}2$, 3 rolls. (*e*) $h = 4{\cdot}4$, 4 rolls. (*f*) $h = 5{\cdot}6$, 5 rolls. (*g*) $h = 6{\cdot}4$, 6 rolls.

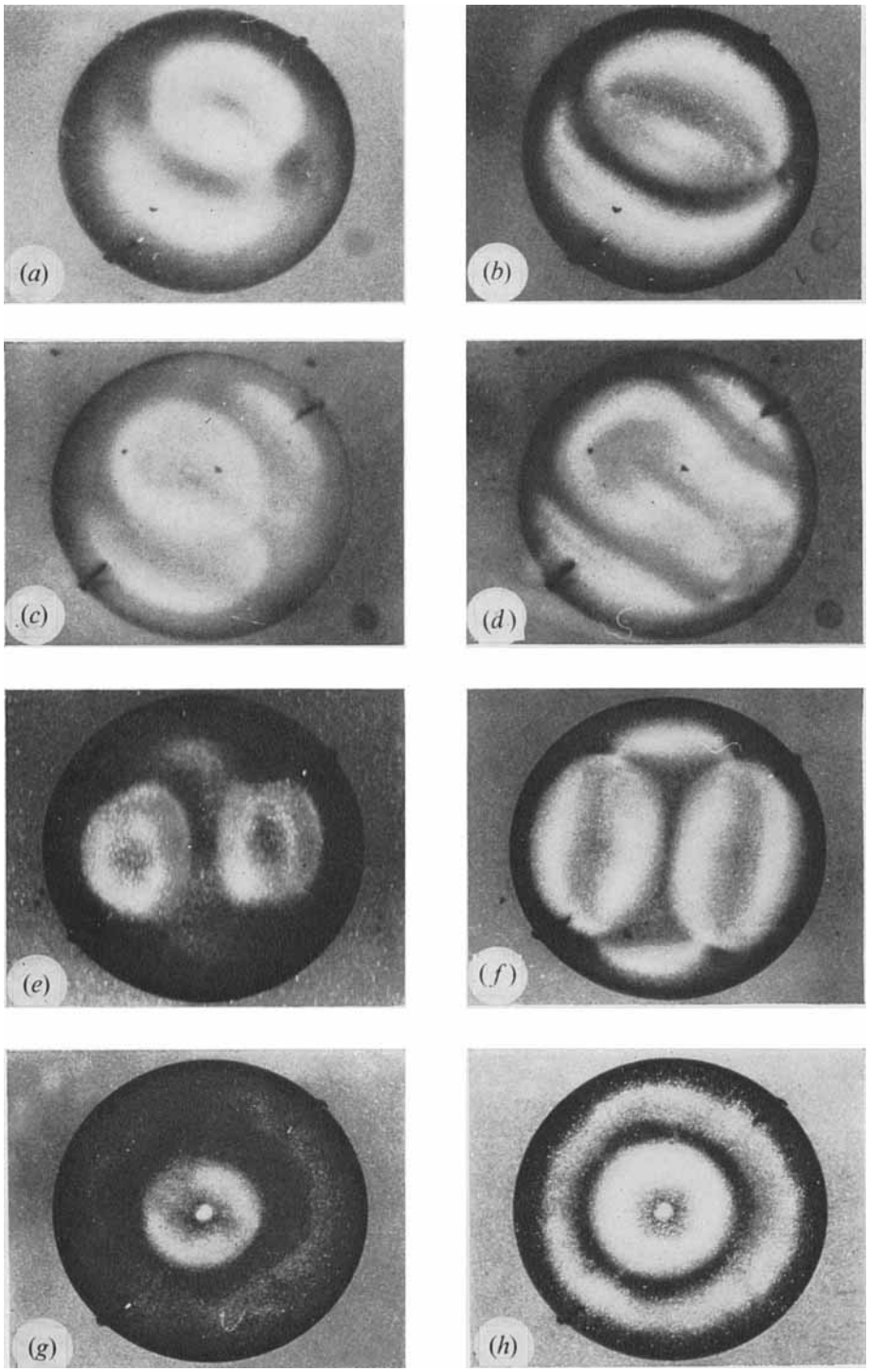

FIGURE 3. Development of different roll configurations owing to different initial conditions. (*a*) (*f*) Critical state. (*a*), (*b*) h = 4·0, 3 rolls; (*b*) 10 min after (*a*). (*c*), (*d*) h = 4·0, 4 rolls; (*d*) 10 min after (*c*). (*e*), (*f*) h = 4·4, 4 rolls; (*f*) 7 min after (*e*). (*g*), (*h*) h = 4·4, 2 ring rolls. (*g*) Convection (Ra = 1100) induced by small horizontal temperature gradients in the centre of the box. (*h*) 2 stable ring rolls at Ra = 1700. (*h*) 35 min after (*g*).

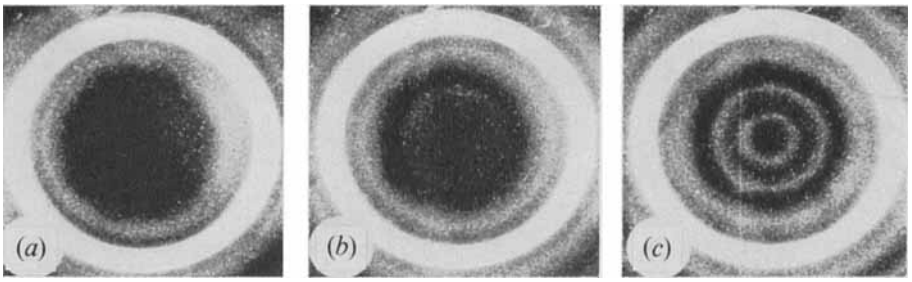

FIGURE 4. Convection rolls in boxes with brass side walls; $h = 7{\cdot}2$. (*a*) Onset of convection; $Ra \approx 170$. (*b*) Second ring roll develops; $Ra \approx 530$. (*c*) Steady convection; $Ra \approx 1000$.

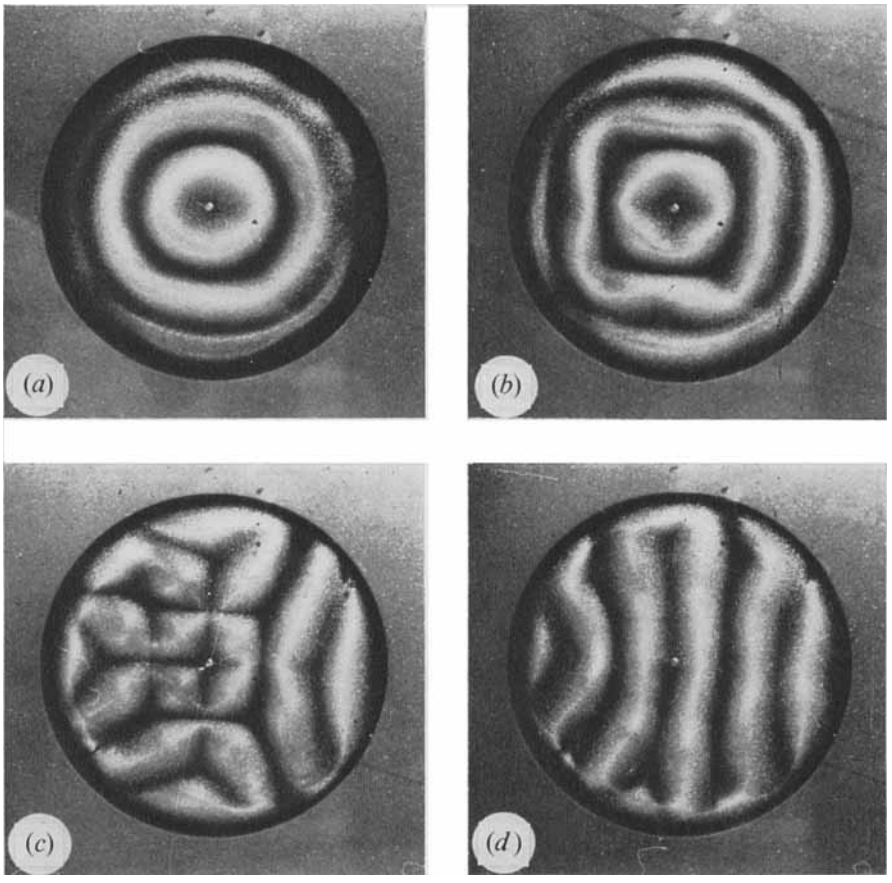

FIGURE 5. Transition from a ring-roll pattern to parallel rolls in a box with $h = 6{\cdot}0$ at the critical state. (*a*) Third ring roll develops near the side wall. (*b*), (*c*) transition to the more stable parallel roll pattern. (*d*) 6 parallel rolls. Time from (*a*) to (*d*) = 2 h.

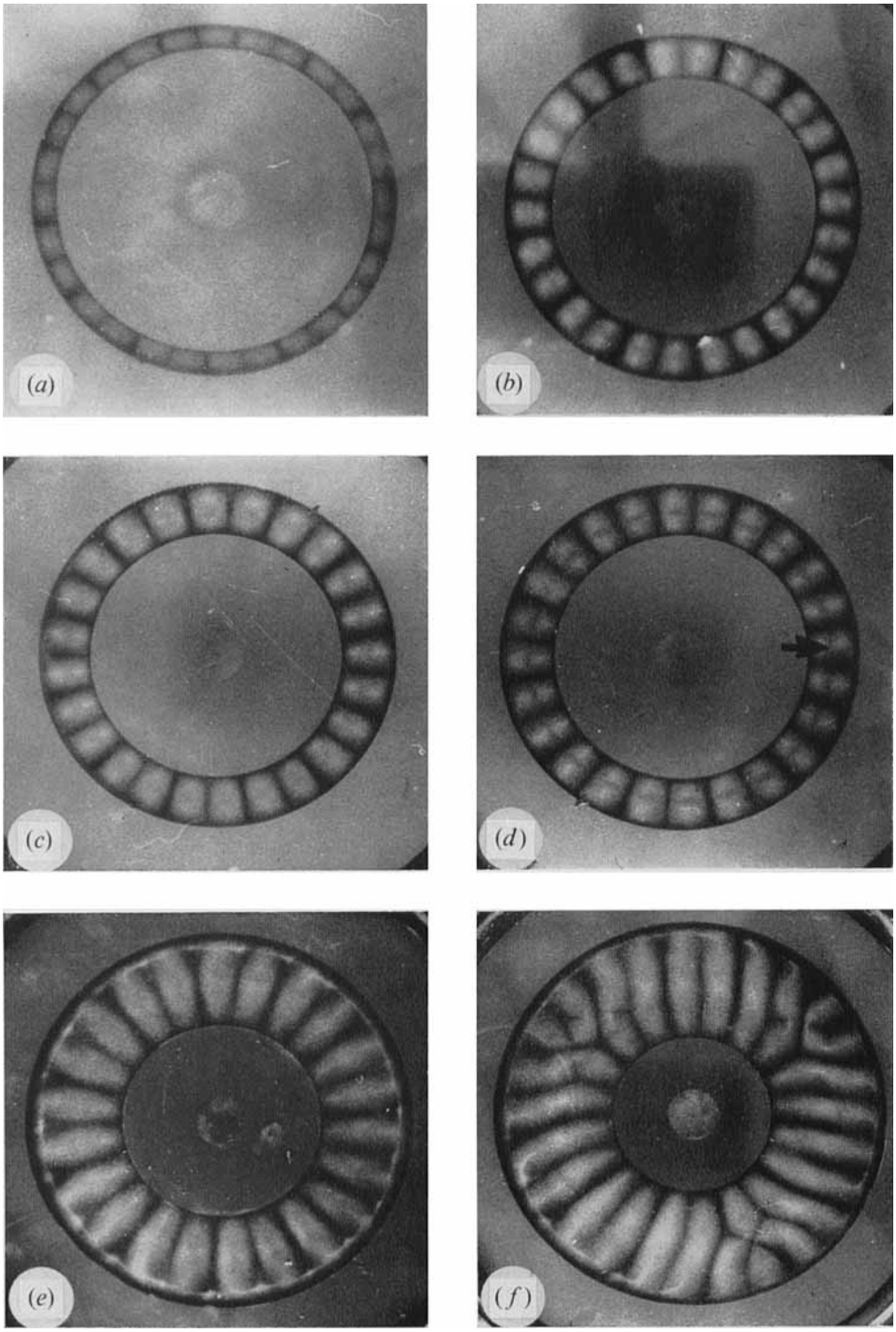

FIGURE 7. Radially directed convection rolls in annuli with insulating side walls. (r_m = 4·0.) (*a*) s = 0·6, 28 rolls. (*b*) s = 1·2, 26 rolls. (*c*) s = 1·4, 24 rolls, 10 min after the onset of convection. (*d*) s = 1·4, 24 rolls divided in the middle (critical conditions), 1½ h after (*c*). (*e*) s = 2·6, 22 rolls with small triangular cells embedded at the outer radius. (*f*) s = 3·4, 20 rolls at the inner and 26 rolls at the outer radius.